J|A|C|S
ARTICLES

Published on Web 12/16/2010

Ruthenium-Decorated Lipid Vesicles: Light-Induced Release of $[Ru(terpy)(bpy)(OH_2)]^{2+}$ and Thermal Back Coordination

Sylvestre Bonnet,*,† Bart Limburg,† Johannes D. Meeldijk,‡ Robertus J. M. Klein Gebbink,§ and J. Antoinette Killian#

Leiden Institute of Chemistry, Gorlaeus Laboratories, Leiden University, P.O. Box 9502, 2300 RA Leiden, The Netherlands, and Electron Microscopy Utrecht, Department of Biology, Organic Chemistry & Catalysis, Debye Institute for Nanomaterial Science, and Biochemistry of Membranes, Bijvoet Center, Department of Chemistry, Faculty of Sciences, Utrecht University, Padualaan 8, 3584 CH Utrecht, The Netherlands

Received June 9, 2010; E-mail: bonnet@chem.leidenuniv.nl

Abstract: Electrostatic forces play an important role in the interaction between large transition metal complexes and lipid bilayers. In this work, a thioether-cholestanol hybrid ligand (**4**) was synthesized, which coordinates to ruthenium(II) via its sulfur atom and intercalates into lipid bilayers via its apolar tail. By mixing its ruthenium complex $[Ru(terpy)(bpy)(\mathbf{4})]^{2+}$ (terpy = 2,2′;6′,2″-terpyridine; bpy = 2,2′-bipyridine) with either the negatively charged lipid dimyristoylphosphatidylglycerol (DMPG) or with the zwitterionic lipid dimyristoylphosphatidylcholine (DMPC), large unilamellar vesicles decorated with ruthenium polypyridyl complexes are formed. Upon visible light irradiation the ruthenium−sulfur coordination bond is selectively broken, releasing the ruthenium fragment as the free aqua complex $[Ru(terpy)(bpy)(OH_2)]^{2+}$. The photochemical quantum yield under blue light irradiation (452 nm) is 0.0074(8) for DMPG vesicles and 0.0073(8) for DMPC vesicles (at 25 °C), which is not significantly different from similar homogeneous systems. Dynamic light scattering and cryo-TEM pictures show that the size and shape of the vesicles are not perturbed by light irradiation. Depending on the charge of the lipids, the cationic aqua complex either strongly interacts with the membrane (DMPG) or diffuses away from it (DMPC). Back coordination of $[Ru(terpy)(bpy)(OH_2)]^{2+}$ to the thioether-decorated vesicles takes place only at DMPG bilayers with high ligand concentrations (25 mol %) and elevated temperatures (70 °C). During this process, partial vesicle fusion was also observed. We discuss the potential of such ruthenium-decorated vesicles in the context of light-controlled molecular motion and light-triggered drug delivery.

Introduction

Over the years ruthenium(II) polypyridyl complexes have become common tools in supramolecular chemistry[1−3] and photochemistry.[4,5] They have also been used in biological environments, either for photosensitizing,[6] for probing the structure of biological membranes,[7,8] for sensing oxygen,[9,10] or as metal drugs.[11,12] Compared to organic luminophores, $[Ru(bpy)_3]^{2+}$ (bpy = 2,2′-bipyridine) shows peculiar photophysical properties, namely, a triplet excited state with a long lifetime and a good resistance toward photobleaching. One of the known mechanisms for the photobleaching of $[Ru(bpy)_3]^{2+}$, though, is the photoejection of one of the bpy chelates.[13,14] This process is caused by the thermal population, from the photogenerated ^{3}MLCT state, of a metal-centered excited state ^{3}MC with strong dissociative character.[15,16] When the ligand field around the ruthenium center is decreased significantly as in $[Ru(terpy)(phen)(L)]^{2+}$ (terpy = 2,2′;6′,2″-terpyridine; phen = 1,10-phenanthroline; L is a sulfoxide, thioether, nitrile, or pyridine monodentate ligand)[17−21] or in the hindered complex $[Ru(bpy)_2(dmbpy)]^{2+}$ (dmbpy = 6,6′-dimethyl-2,2′-bipyridine),[22,23] ligand photoejec-

† Leiden University.
‡ Department of Biology, Utrecht University.
§ Organic Chemistry & Catalysis, Debye Institute for Nanomaterials Science, Utrecht University.
# Biochemistry of Membranes, Bijvoet Center, Department of Chemistry, Utrecht University.

(1) Campagna, S.; Puntoriero, F.; Nastasi, F.; Bergamini, G.; Balzani, V. *Top. Curr. Chem.* **2007**, *280*, 117.
(2) Balzani, V.; Bergamini, G.; Marchioni, F.; Ceroni, P. *Coord. Chem. Rev.* **2006**, *250*, 1254.
(3) Sauvage, J.-P.; Collin, J.-P.; Chambron, J.-C.; Guillerez, S.; Coudret, C. *Chem. Rev.* **1994**, *94*, 993.
(4) Graetzel, M. *Acc. Chem. Res.* **2009**, *42*, 1788.
(5) Concepcion, J. J.; Jurss, J. W.; Brennaman, M. K.; Hoertz, P. G.; Patrocinio, A. O. T.; Murakami Iha, N. Y.; Templeton, J. L.; Meyer, T. J. *Acc. Chem. Res.* **2009**, *42*, 1954.
(6) Park, Y. T.; Noh, S. G. *Int. J. Hydrogen Energy* **1995**, *20*, 789.
(7) Guo, X. Q.; Castellano, F. N.; Li, L.; Lakowicz, J. R. *Biophys. Chem.* **1998**, *71*, 51.
(8) Svensson, F. R.; Li, M.; Norden, B.; Lincoln, P. *J. Phys. Chem. B* **2008**, *112*, 10969.
(9) Cheng, Z.; Aspinwall, C. *Analyst* **2006**, *131*, 236.
(10) McNamara, K. P.; Rosenzweig, N.; Rosenzweig, Z. *Mikrochim. Acta* **1999**, *131*, 57.
(11) Novakova, O.; Kasparova, J.; Vrana, O.; Van Vliet, P. M.; Reedijk, J.; Brabec, V. *Biochemistry* **1995**, *34*, 12369.
(12) Schatzschneider, U. *Eur. J. Inorg. Chem.* **2010**, 1451.
(13) Durham, B.; Walsh, J. L.; Carter, C. L.; Meyer, T. J. *Inorg. Chem.* **1980**, *19*, 860.
(14) Van Houten, J.; Watts, R. J. *J. Am. Chem. Soc.* **1976**, *98*, 4853.
(15) Salassa, L.; Garino, C.; Salassa, G.; Gobetto, R.; Nervi, C. *J. Am. Chem. Soc.* **2008**, *130*, 9590.
(16) Van Houten, J.; Watts, R. J. *Inorg. Chem.* **1978**, *17*, 3381.

 10.1021/ja105025m

tion becomes the most efficient photophysical process, at the cost of luminescence.

In our quest toward the light-controlled motion of single molecules[24,25] we considered investigating the binding and unbinding of ruthenium compounds to and from liposomes in aqueous media. The bilayer of lipid vesicles offers a surface on which metal complexes could eventually move. Meanwhile, their "water solubility" allows for using bulk analytical techniques such as UV−vis spectroscopy to probe the macroscopic state of the system. In addition, vesicles are easy to deposit onto mica or glass, where surface techniques can be used to probe the motion at the single-molecule level.

To date, photosubstitution reactions with ruthenium polypyridyl complexes have mostly been studied in coordinating organic solvents, e.g., acetonitrile or pyridine, or in chlorinated solvents in the presence of chloride anions.[13,17,18,23,26−31] However, several studies have shown that when irradiation is performed in poorly coordinating solvents containing small amounts of water, ruthenium aqua complexes can be formed selectively.[20,32,33] In this article, we consider ligand photosubstitution reactions of $[Ru(terpy)(bpy)(L)]^{2+}$ complexes at the water−bilayer interface, i.e., in buffered aqueous solutions. By covalent linkage of a monodentate ligand L (here a thioether) to a membrane intercalator such as 3β,5α-cholestanol and coordination of the sulfur ligand to ruthenium, we obtained unilamellar vesicles decorated with ruthenium polypyridyl complexes. Visible light irradiation of the vesicles leads to the selective substitution of the monodentate thioether ligand by a water molecule, thus releasing $[Ru(terpy)(bpy)(OH_2)]^{2+}$. The efficiency of this photochemical process at the membrane is not significantly modified compared to comparable homogeneous systems, with a measured photochemical quantum yield of 0.7% at 25 °C under blue light irradiation. With negatively charged lipids, the released aqua complex remains in the vicinity of the membrane through electrostatic interactions, which allows for rebinding to the thioether-decorated vesicles upon heating. Thus, this study paves the way to the light-controlled hopping of ruthenium complexes at a membrane−water interface.

Experimental Section

General. Acetone was dried on potassium carbonate and distilled prior to use. KNO_3 was used as a saturated aqueous solution, and aqueous KPF_6 was 40 g L^{-1}. ^1H (300.1/400.0 MHz) and ^{13}C (75.5/100.6 MHz) NMR spectra were recorded on a Varian INOVA 300 MHz or 400 MHz spectrometer; $^{31}P\{^1H\}$ (121.5 MHz) and ^{19}F (376 MHz) NMR spectra were recorded on a Varian INOVA 400 MHz spectrometer. Chemical shift values are reported in ppm (δ) relative to Me_4Si (^1H and ^{13}C NMR). MS measurements were carried out on an Applied Biosystems Voyager DE-STR MALDI-TOF MS. Elemental analyses were performed by H. Kolbe Microanalysis Laboratories, Mülheim, Germany. UV−vis absorption spectra were taken on a Cary 5 spectrophotometer from Varian. For column chromatography, Merck silica gel 60 (230−400 mesh) was used. All standards reagents were purchased from Acros Organics and Aldrich Chemical Co. Inc. and used as received. $[Ru(terpy)(bpy)(OH_2)](BF_4)_2$[34] and $[Ru(terpy)(bpy)(Cl)](Cl)$[34] were obtained as described in the literature. Cholesterol, bromoacetylchloride, sodium thiomethoxide, and acetic acid were from commercial sources and used as received. 1,2-Dimyristoyl-*sn*-glycero-3-phosphoglycerol (DMPG) and 1,2-dimyristoyl-*sn*-glycero-3-phosphocholine (DMPC) were obtained from Avanti Polar Lipids and stored at −18 °C. A chloride-free buffer solution was prepared by mixing KH_2PO_4 (313 mg, 2.3 mmol), $K_2HPO_4 \cdot 3H_2O$ (593 mg, 2.6 mmol), and K_2SO_4 (849 mg, 4.87 mmol) in a 500-mL volumetric flask and dissolving with Milli-Q water (pH = 7.03 at 23 °C). All photosensitive solutions were protected from light by aluminum foil.

Synthesis. Compound **2** was obtained by hydrogenation of cholesterol. To a solution of **1** (7.73 g, 20 mmol) in tetrahydrofuran (20 mL) were added palladium on charcoal (400 mg, 10%) and acetic acid (1.7 mL). This mixture was transferred in a Parr apparatus and subjected to hydrogenation at 60 °C under 5 bar of H_2 until consumption of H_2 ceased (∼45 min). The cooled mixture was filtered on Celite, the Celite was washed twice with THF (30 mL), the gathered organic phase evaporated to dryness, and the crude product recrystallized from hot hexane (30 mL) down to 4 °C to give 5α-cholestan-3β-ol (compound **2**, 5.90 g, 76%).

Compound 3. To a solution of **2** (5.90 g, 15.2 mmol) in dry tetrahydrofuran (100 mL) was added bromoacetylchloride (4.5 mL, 53.1 mmol). The solution was heated to reflux for 2 h, the solvent was evaporated on a rotary evaporator, and the minimum amount of hot hexane was added to dissolve the crude product. After cooling down to room temperature the hexane solution was left in the fridge overnight to yield after filtration and drying bromoacetyl 5α-cholestan-3β-oate as a pale green crystalline solid (compound **3**, 5.48 g, 71%). ^1H NMR (400 MHz, δ in $CDCl_3$): 4.75 (m, 1H, CHOCO), 3.79 (s, 2H, CH_2Br), 1.97 (dt, 1H, J = 3.3, 12.4), 1.90−0.90 (m, 29H), 0.89 (d, 3H, J = 6.5), 0.87 (d, 3H, J = 6.6), 0.85 (d, 3H, J = 6.6), 0.82 (s, 3H), 0.65 (s+m, 4H). ^{13}C NMR (101 MHz, δ in $CDCl_3$): 166.92, 77.48, 77.16, 76.84, 76.13, 56.54, 56.41, 54.32, 44.76, 42.73, 40.11, 39.66, 36.80, 36.31, 35.94, 35.60, 35.58, 33.83, 32.10, 28.72, 28.38, 28.15, 27.35, 26.58, 24.34, 23.98, 22.96, 22.71, 21.36, 18.82, 12.37, 12.21. ESI MS exp (calcd): 531.26 (531.28, $[M + Na]^+$), 1041.4 (1041.6, $[2M + Na]^+$), 1551.4 (1551.9, $[3M + Na]^+$). C,H,N expt 68.45/9.75/0.00; calcd 68.35/9.69/0.0 for $C_{29}H_{49}BrO_2$.

Compound 4. Compound **3** (1.02 g, 2.0 mmol) and sodium thiomethoxide (289 mg, 4.12 mmol) were weighed in a round-bottom flask and put under N_2. Dry tetrahydrofuran (50 mL)was cannulated under N_2, and the suspension was heated to reflux for 2 h. THF was removed under vacuum, 100 mL of water was added, and the product was extracted with Et_2O (3 × 75 mL). The

(17) Hecker, C. R.; Fanwick, P. E.; McMillin, D. R. *Inorg. Chem.* **1991**, *30*, 659.
(18) Bonnet, S.; Collin, J.; Sauvage, J.; Schofield, E. *Inorg. Chem.* **2004**, *43*, 8346.
(19) Bonnet, S.; Collin, J.-P.; Gruber, N.; Sauvage, J.-P.; Schofield, E. R. *Dalton Trans.* **2003**, 4654.
(20) Bonnet, S.; Collin, J.; Sauvage, P. *Inorg. Chem.* **2006**, *45*, 4024.
(21) Bonnet, S.; Collin, J.-P.; Sauvage, J.-P. *Inorg. Chem.* **2007**, *46*, 10520.
(22) Laemmel, A.; Collin, J.; Sauvage, J. *Eur. J. Inorg. Chem.* **1999**, 383.
(23) Mobian, P.; Kern, J.-M.; Sauvage, J.-P. *Angew. Chem., Int. Ed.* **2004**, *43*, 2392.
(24) Bonnet, S.; Collin, J.; Koizumi, M.; Mobian, P.; Sauvage, J. *Adv. Mater.* **2006**, *18*, 1239.
(25) Bonnet, S.; Collin, J.-P. *Chem. Soc. Rev.* **2008**, *37*, 1207.
(26) Rillema, D. P.; Blanton, C. B.; Shaver, R. J.; Jackman, D. C.; Boldaji, M.; Bundy, S.; Worl, L. A.; Meyer, T. J. *Inorg. Chem.* **1992**, *31*, 1600.
(27) Laemmel, A.; Collin, J.; Sauvage, J. *C. R. Acad. Sci., Ser. IIc: Chim.* **2000**, *3*, 43.
(28) Baranoff, E.; Collin, J.-P.; Furusho, Y.; Laemmel, A.-C.; Sauvage, J.-P. *Chem. Commun.* **2000**, 1935.
(29) Collin, J.-P.; Laemmel, A.-C.; Sauvage, J.-P. *New J. Chem.* **2001**, *25*, 22.
(30) Collin, J.; Jouvenot, D.; Koizumi, M.; Sauvage, J. *Inorg. Chem.* **2005**, *44*, 4693.
(31) Collin, J.-P.; Jouvenot, D.; Koizumi, M.; Sauvage, J.-P. *Inorg. Chim. Acta* **2007**, *360*, 923.
(32) Ossipov, D.; Gohil, S.; Chattopadhyaya, J. *J. Am. Chem. Soc.* **2002**, *124*, 13416.
(33) Schofield, E.; Collin, J.; Gruber, N.; Sauvage, J. *Chem. Commun.* **2003**, 188.
(34) Takeuchi, K. J.; Thompson, M. S.; Pipes, D. W.; Meyer, T. J. *Inorg. Chem.* **1984**, *23*, 1845.

combined ether fractions were washed with water and brine, dried with $MgSO_4$, filtered, and evaporated to dryness. Column chromatography on silica gel (200 mL) using pentane/dichloromethane mixtures (8:3 to 1:1) afforded ligand **4** as a white solid (785 mg, 82%). ^{1}H NMR (400 MHz, δ in $CDCl_3$): 4.74 (m, 1H, 3⟨), 3.14 (s, 2H, SCH_2O), 2.20 (s, 3H, CH_3S), 2.0−0.93 (m, 25H), 0.89 (d, 3H), 0.85 (dd, 6H), 0.82 (s+m, 4H). ^{13}C NMR (100.6 MHz, δ in $CDCl_3$): 169.95 (COO), 74.93 ($CH^{(}O$), 56.54, 56.41, 54.34, 44.80, 42.72, 40.11, 39.65, 36.86, 36.30, 36.15, 35.93, 35.60, 34.09, 32.12, 28.74, 28.38, 28.14, 27.58, 24.34, 23.98, 22.96, 22.70, 21.35, 18.81, 16.37, 12.38, 12.21. ESI MS exp (calc): 499.355 (499.359, $[M + Na]^+$), 975.67 (975.72, $[2M + Na]^+$), 1451.8 (1452.1, $[3M + Na]^+$). C,H,N expt 75.69/11.00/0.00; calc 75.57/10.99/0.0 for $C_{30}H_{52}O_2S$.

[5](PF$_6$)$_2$. [Ru(terpy)(bpy)(Cl)](Cl) (150 mg, 0.27 mmol) and ligand **4** (138 mg, 0.29 mmol) were weighed in a round-bottom flask and put under N_2. Dry, degassed acetone was added (20 mL), and an acetone solution of $AgBF_4$ (113 mg, 0.58 mmol) was cannulated under N_2. The reaction mixture was heated at reflux overnight (16 h), cooled to room temperature, and filtered over Celite, and acetone was removed under vacuum. The crude product was purified by chromatography on silica gel (200 mL) using an acetone/water/KNO_{3sat} mixture (100:10:1). The bright orange fraction was collected, 50 mL of aqueous KPF_6 was added, acetone was removed on a rotary evaporator, and the precipitate was filtered on a glass filter, washed thoroughly with water and Et_2O, and dried under vacuum. Yield: 94 mg of compound **4** as a bright orange solid (50%). ^{1}H NMR (400 MHz, δ in acetone-d_6): 10.1 (dd, 1H, A2), 8.94 (d, 3H), 8.74 (d, 2H), 8.71 (d, 1H), 8.52 (m, 2H), 8.20 (m, 3H), 8.01 (m, 3H), 7.53 (m, 3H), 7.31 (m, 1H), 4.45 (m, 1H, CHO), 3.00 (s, 2H, SCH_2O), 1.62 (s, 3H, CH_3S), 2.02−0.82 (m, 39H), 0.78 (s, 3H), 0.67 (s+m, 4H). ^{13}C NMR (100.6 MHz, δ in acetone-d_6): 166.9, 159.1, 158.4, 157.74, 157.66, 154.7, 153.3, 150.9, 140.0, 139.3, 138.2, 129.5, 128.7, 128.3, 126.1, 125.7, 125.4, 124.9 (18 C_{arom}), 76.5 (CH_2O), 57.28, 57.15, 55.01, 45.24, 43.35, 40.84, 40.23, 37.24, 36.92, 36.89, 36.58, 36.25, 36.08, 34.52, 32.69, 29.22, 28.89, 28.67, 27.95, 24.83, 24.51, 23.06, 22.82, 21.89, 19.07, 15.58, 12.46, 12.41 (SMe + 27 C_{alkyl}). ^{19}F NMR (376.3 MHz, δ in acetone-d_6): −72.9 (d, J_{F-P} = 707.8 Hz). UV−vis: λ_{max} in nm (ε in cm M^{-1}): 454 (7760), 328 (15900), 332 (15900). ESI MS exp (calc): 483.709 (483.719 for $C_{57}H_{75}N_5O_3RuS$, $[M - 2PF_6]^{2+}$). C,H,N expt 52.59/5.69/5.32; calcd 52.54/5.69/5.57 for $C_{55}H_{71}F_{12}N_5O_2P_2RuS$.

Vesicle Preparation. Aliquots of phospholipids (0.005 mmol) and ligand **4** or complex [**5**](PF$_6$)$_2$ (1−25 mol %, see Table 1) were mixed from chloroform stock solutions and dried under a flow of nitrogen for a few hours. They were subsequently placed under vacuum to remove traces of chloroform. Then the lipid mixtures were hydrated in a chloride-free buffer containing 10 mM of phosphates and 40 mM of K_2SO_4 (total ionic strength 50 mM), at pH = 7.0. The final concentration of the lipids was 2.5 mM. The lipid suspensions were freeze−thawed 10 times (from liquid N_2 temperature to +50 °C) and then extruded 10 times (at +50 °C) through 200 nm polycarbonate filters. The vesicle-containing samples were conserved in the dark at 4 °C and used within 5 days.

Dynamic Light Scattering. Vesicle size was determined by dynamic light scattering in a Zetasizer (Malvern Instruments Ltd., U.K.), operated at a wavelength of 633 nm.

Cryo-transmission Electron Microscopy. A 3-μL aliquot of sample solution was pipetted onto a glow discharged Quantifoil R2/2 copper grid 200 mesh in the environmental chamber of a Vitrobot with a RH of 100% at 30 °C. The sample was blotted once during 2 s and plunged into liquid ethane. The grid was transferred to a Gatan cryoholder Model 626. The transmission electron microscope used was a Philips Tecnai12 equipped with a Biotwin-lens and a W filament, operated at 120 kV acceleration voltage. Images were captured with a SIS Megaview II CCD-camera and processed with iTEM software.

Irradiation and Quantum Yield Measurement. White light irradiations were performed using the 150 W halogen lamp of a microscope; the sample to irradiate was placed in a water bath at 25 °C to filter IR and UV radiations, and the reaction was followed by UV−vis spectroscopy. For quantum yield determination the continuous beam of a 1000 W xenon arc lamp from Lot was filtered by a water filter of 15 cm diameter followed by an Andover 452FS10-50 interference filter from Lot Oriel (λ_{ex} = 452 nm). Samples (3 mL) containing the vesicles (1.25 mM) functionalized with 5 mol % of [**5**](PF$_6$)$_2$ were put in a closed, UV−vis quartz cell (path length 1 cm) under an air atmosphere and stirred in a water bath at 25 °C. Under these conditions, a light intensity of $6.4(3) \times 10^{-8}$ einstein s^{-1} was measured using standard ferrioxalate actinometry (see Supporting Information).[35] The extinction coefficients of $[Ru(terpy)(bpy)(OH_2)]^{2+}$ at the excitation wavelength (452 nm) and in the presence of the ligand-functionalized vesicles were determined by adding known amounts of the complex to vesicle solutions containing 5 mol % of ligand **4** (values found: ε_{452} = 10800 cm M^{-1} for DMPG and 9750 cm M^{-1} for DMPC). From the evolution of the UV−vis spectra of the vesicle-containing solution (see Supporting Information), the variation of C_t, the concentration in [**5**]$^{2+}$, was determined as a function of irradiation time t, and a linear regression of $\ln(C_t/C_0)$ as a function of t gave a pseudo-first-order rate constant of 2.34×10^{-3} s^{-1} for DPMG and 2.27×10^{-3} s^{-1} for DPMC. The quantum yield for the photosubstitution of ligand **4** by H_2O at vesicles was calculated to be 0.0074(8) for DMPG and 0.0073(8) for DMPC.

Ultracentrifugation. The UV−vis spectrum of a freshly prepared vesicle sample was first measured between 250 and 800 nm. A 1.0-mL sample was ultracentrifuged at 25 °C and 100 krpm (RCF 35 500 g) for 1 h. Next, 0.70 mL of the supernatant was pipetted out, and its UV−vis spectrum was measured. The lipid content of the supernatant was measured by a Rouser assay[36] after Bligh and Dyer extraction.[37] The Bligh and Dyer method was used to extract the phospholipids from the aqueous phase as follows. To each sample (0.4 mL) were added methanol (1.2 mL) and chloroform (0.5 mL), and the mixture was homogenized. It was then extracted 3 times by addition of chloroform (0.5 mL), mixing, centrifugation at 3000 rpm (RCF 1620g) for 3 min, and removal of the chloroform phase. The combined organic fractions were evaporated under a flow of N_2 for 1 h, and dried under vacuum for 30 min. The Rouser assay consists of a spectrophotometric titration of the phosphate concentration using a molybdate salt. Each extracted sample was decomposed with $HClO_4$ (0.3 mL, 70−72%) at 180 °C for 1 h. After cooling of the samples to room temperature, water (1 mL) was added, followed by ammonium heptamolybdate (0.4 mL, 1.25% w/v) and ascorbic acid (0.4 mL, 5% w/v), and the samples were cooked 5 min in boiling water, using marbles as stoppers to prevent evaporation. The absorbance of the solution at 797 nm was measured and compared to a calibration curve obtained using 6 samples containing 0, 10, 20, 30, 40, 50 nmol of phosphate and prepared in exactly the same conditions. Typical linear regression coefficients R^2 = 0.9997 were found, and the amount of lipids found in the supernatant after ultracentrifugation was calculated accordingly.

Results

Ligand Synthesis and Coordination to Ruthenium. The three-step synthesis of ligand **4** is shown in Scheme 1: hydrogenation of cholesterol was achieved first, followed by esterification with bromoacetylchloride, and nucleophilic substitution of the bromide by a methanethiolate group. Coordination of **4** to ruthenium was realized by reacting it with [Ru(terpy)(bpy)(Cl)](Cl) in the presence of 2 equiv of $AgBF_4$ in acetone, followed by column chromatography (see Scheme 2). Anion

(35) Calvert, J. G.; Pitts, J. N., Chemical actinometer for the determination of ultraviolet light intensities. In *Photochemistry*; Wiley and Sons: New York, 1967; pp 780.
(36) Rouser, G.; Fleische, S.; Yamamoto, A. *Lipids* **1970**, *5*, 494.
(37) Bligh, E. G.; Dyer, W. J. *Can. J. Biochem. Physiol.* **1959**, *37*, 911.

Scheme 1. Synthesis of Ligand **4**

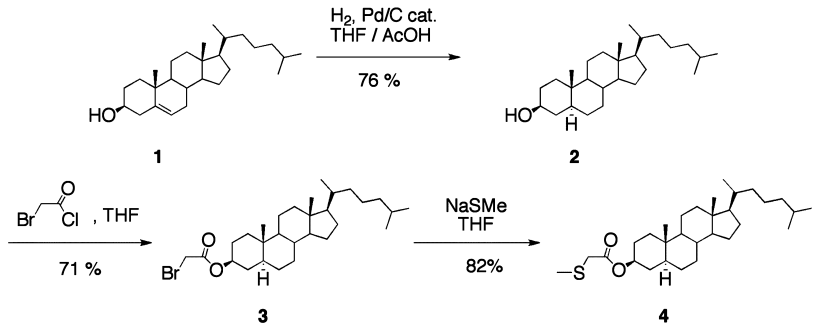

Scheme 2. Synthesis of Complex [**5**](PF$_6$)$_2$ and Notation of the Protons

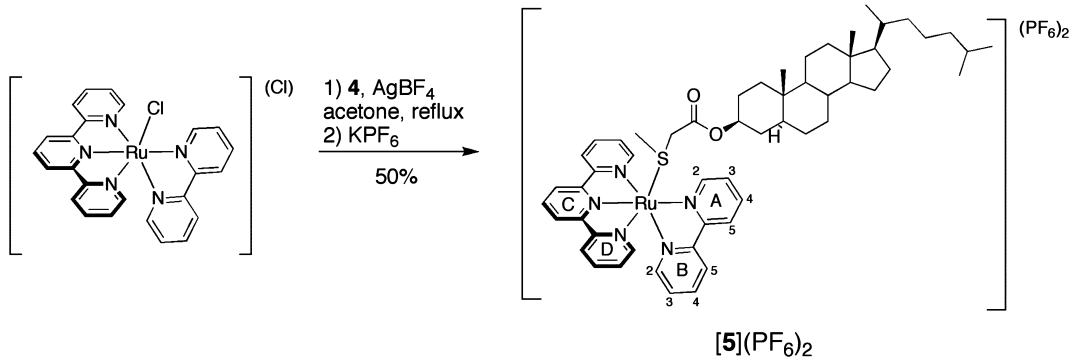

exchange using KPF_6 in excess yielded the water-insoluble orange complex [**5**](PF$_6$)$_2$, which was characterized by ^{1}H, ^{19}F, and ^{13}C NMR, mass spectrometry (ESI-MS), elemental analysis, and UV−vis spectroscopy. Coordination of the sulfur atom of **4** to the ruthenium atom in complex [**5**](PF$_6$)$_2$ is characterized by an absorption maximum at 454 nm in acetone,[38,39] as well as by a low-field shifted doublet for the A2 proton on the bipyridine in ^{1}H NMR spectroscopy (10.1 ppm in acetone-d_6, see Scheme 2 for notations).[40]

Vesicle Preparation and Characterization. Large unilamellar vesicles (LUVs) including 1 mol % of either complex [**5**](PF$_6$)$_2$ or ligand **4** were prepared as described (see Experimental Section). Eight types of samples were prepared as indicated in Table 1. Although [**5**](PF$_6$)$_2$ is not water-soluble, upon incorporation into the vesicles transparent yellow suspensions were obtained for sample C and F (i.e., those containing 1 mol % of [**5**](PF$_6$)$_2$). The UV−vis spectrum of the vesicle solutions showed the characteristic weak ^{3}MLCT absorption bands of [**5**]$^{2+}$ in the visible region (absorption maximum at 450 nm) and several more intense bands in the UV region (see Figure 1).

The size distribution of the vesicles was measured by dynamic light scattering (see Table 1). A narrow distribution centered between 140 and 180 nm was obtained, which is consistent with the nominal size of the filter holes used in the preparation (ϕ 200 nm). In order to obtain more insight into the morphology of the vesicles, cryo-transmission electron microscopy (cryo-TEM) was performed by vitrification above T_m on samples A−F (see Figure 2).

Table 1. Composition of Samples A−F and Characterization by Dynamic Light Scattering

sample	lipid[a]	additive[b,c]	$Z_{average}$ (nm)	polydispersity index
A	DMPG		140.9 ± 6.1	0.038 ± 0.043
B	DMPG	**4**	156.3 ± 4.6	0.113 ± 0.059
B′	DMPG	**4** + [Ru-OH$_2$]$^{2+}$	156.3 ± 4.6	0.113 ± 0.059
C	DMPG	[**5**]$^{2+}$	160.1 ± 3.7	0.156 ± 0.030
C irradiated	DMPG	[**5**]$^{2+}$ + hν	167.8 ± 3.8	0.114 ± 0.034
D	DMPC		169.9 ± 7.2	0.070 ± 0.034
E	DMPC	**4**	177.8 ± 1.8	0.097 ± 0.032
E′	DMPC	**4** + [Ru-OH$_2$]$^{2+}$	177.8 ± 1.8	0.097 ± 0.032
F	DMPC	[**5**]$^{2+}$	155.1 ± 2.0	0.093 ± 0.033
F irradiated	DMPC	[**5**]$^{2+}$ + hν	155.7 ± 3.4	0.109 ± 0.024

[a] Lipid concentration is 2.5 mM. [b] Unless otherwise noted, additives are introduced with a concentration of 1 mol % compared to the lipids. [c] [Ru-OH$_2$]$^{2+}$ stands for [Ru(terpy)(bpy)(OH$_2$)](BF$_4$)$_2$ and is added *after* preparation of the vesicles.

With anionic lipids (DMPG, samples A−C, see Figure 2) a relatively low concentration of vesicles was observed on the negatively charged support, probably due to repulsive electrostatic interactions. Samples of type A and B contained only unilamellar vesicles with a size compatible with DLS measurements (∼150 nm). Sample C also contained unilamellar vesicles, but another type of structure was observed as well, which appeared as dark lines, ovoids, or discs with a uniform contrast (see black arrow in Figure 2c). Finally some of these unilamellar vesicles appeared faceted or as open bilayer fragments. On average, the diameter of the particles is roughly ∼150 nm, which is consistent with DLS measurements. The bilayer thickness was 7 ± 1 nm, which corresponds to the expected value for a single bilayer. Pixel size of the images was in the range of 1 nm, which limited the accuracy of the measurements.

When neutral DMPC lipids were used (samples D−F) a much higher number of vesicles was observed (see Figure 2d−f), as

(38) Root, M. J.; Deutsch, E. *Inorg. Chem.* **1985**, *24*, 1464.
(39) Bonnet, S.; Collin, J.; Gruber, N.; Sauvage, J.; Schofield, E. *Dalton Trans.* **2003**, 4654.
(40) The chemical shift of the A2 proton is very sensitive to the nature of the monodentate ligand coordinated to ruthenium. For example, in D_2O the A2 proton of [Ru(terpy)(bpy)(Cl)]$^+$ appears at 9.93 ppm, that of [Ru(terpy)(bpy)(OH$_2$)]$^{2+}$ at 9.55 ppm, and that of [Ru(terpy)(bpy)(2-thiomethoxyethanol)]$^{2+}$ at 9.80 ppm (unpublished results).

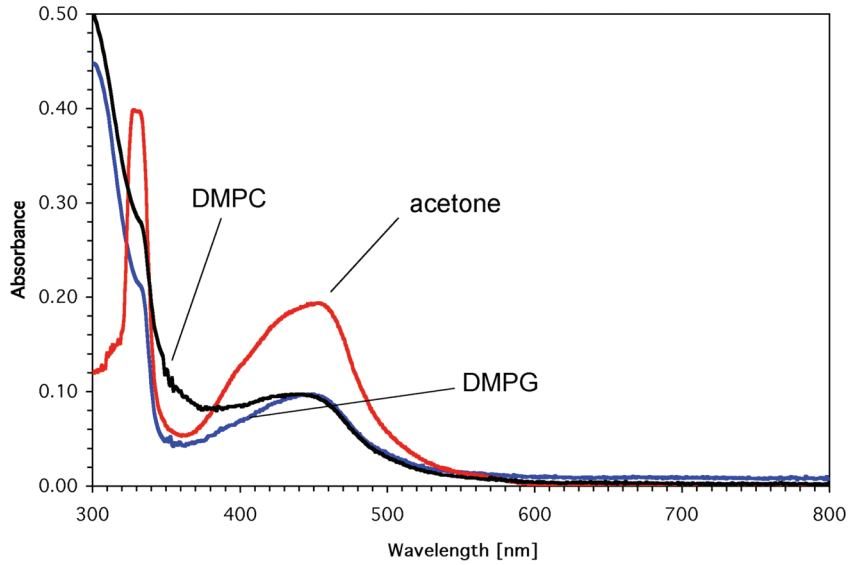

Figure 1. UV−vis spectra of [**5**]$(PF_6)_2$ (0.025 mM) in acetone, DMPG vesicles, and DMPC vesicles.

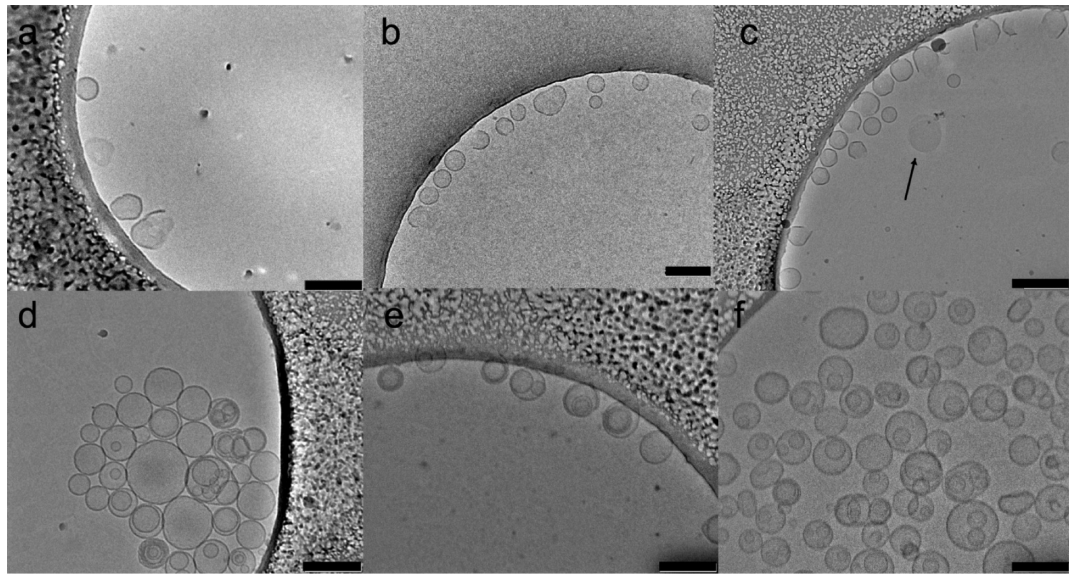

Figure 2. Cryo-TEM pictures of samples A−F. In each picture the scale bar is 200 nm. For sample C the black arrow shows the uniform disk mentioned in the text.

there was no repulsive interaction with the negatively charged carbon support. Although the vesicles were mostly unfaceted and unilamellar, a significant number of multilamellar vesicles were also present. Contrary to DMPG samples no uniform discs were observed. The size of the vesicles was consistent with the DLS measurements (∼50−200 nm), and the bilayer thickness was 7 ± 1 nm.

Irradiation Experiments. When the ruthenium-functionalized vesicles (samples C and F) are irradiated with white light at 25 °C, a gradual color change from yellow to red is observed. At any point of the experiment if the irradiation is stopped the spectrum of the solution also stops evolving, which shows the thermal inertness of the ruthenium complex in the dark. Figure 3a shows the evolution of the UV−vis spectrum of sample C as a function of irradiation time. Clear isosbestic points are observed at 458, 386, 332, 311, 297, and 288 nm, showing that a single photoreaction is taking place. The initial absorption band at 457 nm gradually vanishes to give rise to a new species characterized by an absorption band at 492 nm. The absorption spectrum in the end of the photoreaction is very close to that of sample B′, in which $[Ru(terpy)(bpy)(OH_2)]^{2+}$ was added to vesicles functionalized with ligand **4** (see Figure 3b). It is also close to that of $[Ru(terpy)(bpy)(OH_2)]^{2+}$ in water; we attribute the small differences between vesicle-containing and vesicle-free samples to the interaction between the aqua complex and the membrane. Similar results were obtained with DMPC vesicles: the UV−vis spectrum of sample F after irradiation was found nearly identical to that of sample E′ (data not shown).

As shown in the insert of Figure 3a, a pseudo-first-order kinetics is observed for the photoreaction using white light ($\ln(C_t/C_0) = -kt$, where C_0 and C_t are the concentration of $[\mathbf{5}]^{2+}$ before irradiation and after an irradiation time t, respectively). The quantum yield of the process was measured at 25 °C using monochromatic light set at the wavelength of the isosbestic point (λ_{ex} = 452 nm). In the conditions of the experiment (see Experimental Section), the quantum yield for the photosubstitution of **4** by an aqua ligand at the ruthenium center was found to be 0.0074(8) for DMPG and 0.0073(8) for DMPC vesicles.

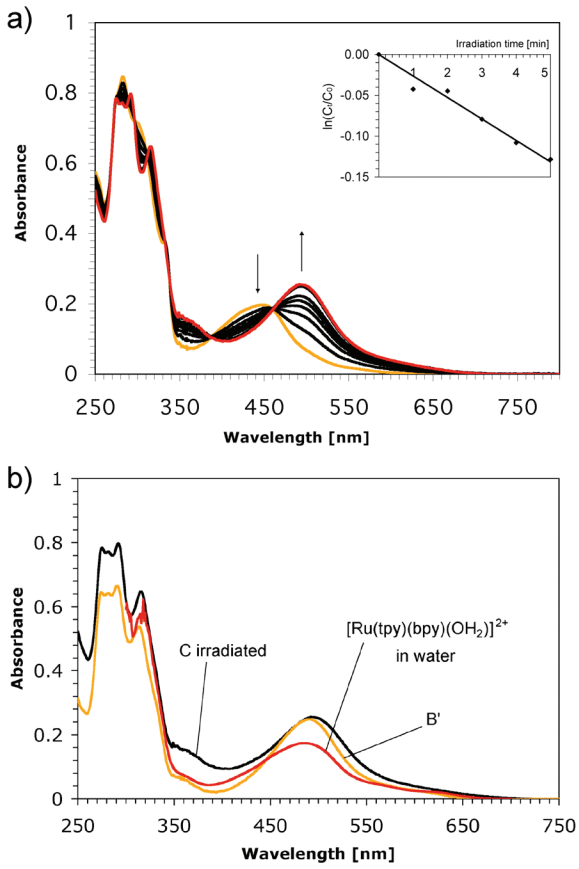

Figure 3. (a) Evolution of the UV−vis spectrum of sample C upon white light irradiation at 25 °C in a pH = 7.0, chloride-free phosphate buffer (t = 0, 1, 2, 3, 4, 5, 10, and 15 min). Insert shows the evolution of $\ln(C_t/C_0)$ as a function of irradiation time t, where C_t and C_0 stand for the concentration of $[\mathbf{5}]^{2+}$ at time t and $t = 0$, respectively. (b) Superimposed UV−vis spectra of sample C after irradiation (black), sample B′ (orange), and a reference sample of $[Ru(terpy)(bpy)(OH_2)](BF_4)_2$ in water (red).

These values are of the same order of magnitude as the ones published for nitrile ligands,[17,18] which highlights that the membrane environment does not significantly modify the photosubstitution properties of the ruthenium complex.

For samples C and F, cryo-electron microscopy shows that the morphology of the ruthenium-functionalized vesicles after visible light irradiation is very similar to that before irradiation (see Figure 4). For sample C (DMPG, Figure 4 left), unfaceted unilamellar vesicles were observed, as well as uniform discs

Table 2. Absorption Maximum of the Solution before Ultracentrifugation and Color of the Lipid Pellets after Centrifugation for Samples A−F[a]

sample	λ_{max} of solution before ultracentrifugation (nm)	Color of pellet after ultracentrifugation
A, B	n.o.	colorless[b]
B′	492	red
C	454	yellow
C irradiated	492	red
D, E	n.o.	colorless[b]
E′	492	colorless[b]
F	454	yellow
F irradiated	492	colorless[b]

[a] n.o. = not observed. [b] The colorless pellets were not fully transparent and slightly diffused light.

(see below). The size of the particles ranged between 100 and 200 nm. For sample F (DMPC, Figure 4 right), a mixture of unilamellar, multilamellar, and vesicular vesicles was found after irradiation, with sizes of 50−200 nm. DLS measurement of the vesicles led to the same conclusion (see Table 1): visible light irradiation neither alters the size, nor the shape of the ruthenium-functionalized vesicles C and F, and leads to a state that is similar to sample B′ and E′ (see Discussion).

Ultracentrifugation Experiments. Samples C and F were subjected to ultracentrifugation, before and after irradiation. The absorbance of the supernatant was quantitatively measured at the absorption maximum of the ruthenium complex (454 nm before irradiation and 492 nm after, see Table 2) and compared to the absorbance before centrifugation (see Table 3).

With both DMPG and DMPC vesicles, the pellets obtained by ultracentrifugation before irradiation are yellow, and the absorbance of the supernatant is low, thus showing attachment of the ruthenium complex to the lipid vesicles. After irradiation the situation is more contrasted (see Tables 2 and 3): for anionic DMPG vesicles red pellets are observed, and according to the UV−vis spectrum of the supernatant only ∼15% of the initial absorbance is retained. Thus, ∼85% of the photochemically produced $[Ru(terpy)(bpy)(OH_2)]^{2+}$ complexes are contained in the pellet. On the contrary, for neutral DMPC vesicles the lipid pellets obtained after ultracentrifugation are colorless, and the absorbance at 492 nm is identical before and after centrifugation. Thus, in this case the released $[Ru(terpy)(bpy)(OH_2)]^{2+}$ is essentially noninteracting with the lipid bilayer.

For sample B′ and E′, after ultracentrifugation the pellets were found red and colorless, respectively (see Table 2), and the supernatant showed similarly low (16%) and high (75%)

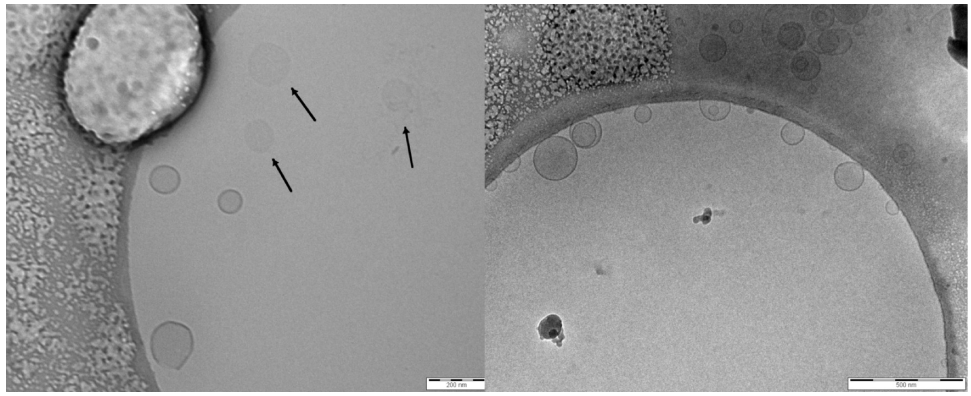

Figure 4. Cryo-TEM pictures of sample C (left) and F (right) after visible light irradiation. For sample C, black arrows show the uniform discs also seen before irradiation (see Figure 2C).

Table 3. Percentages of Immobilization of Ruthenium at DMPG and DMPC Vesicles before and after Irradiation

	absorbance at λ_{max}			
sample	before centrifugation	after centrifugation	remaining Ru in supernatant (%)[c]	remaining lipid in supernatant (%)[d]
A′ [a]	0.292	0.050	17	<0.8
B′	0.282	0.045	16	<2.1
C irradiated	0.314	0.044	14	<1.8
C	0.239	0.059	25	<1.4
D′ [a]	0.273	0.283	103[b]	<0.3
E′	0.350	0.262	75	<0.2
F irradiated	0.258	0.277	107[b]	<0.1
F	0.226	0.126	56	<0.1

[a] Obtained by adding 1 mol % of $[Ru(terpy)(bpy)(OH_2)](BF_4)_2$ to sample A (A′) or D (D′). [b] With DMPC samples (D′, E′, F, and F irradiated) light scattering was found to be large, which significantly increased the absorbance of the baseline and hence the errors during application of the Beer−Lambert law. Estimated absolute errors on these values are 10−20%. [c] According to UV−vis spectroscopy. [d] According to Rouser assays.

ruthenium content, which is comparable to sample C and F after irradiation (see Table 3). In all cases, a Rouser assay showed that the supernatant did not contain significant amounts of lipids, as the phosphate content was lower than 2% (see Table 3).

Back-Coordination. After irradiation, samples C and F were heated at 60 °C for several hours, and up to 80 °C overnight (16 h). The same heat treatment was applied to sample B′ and E′. In all cases, the UV−vis spectrum after heating showed a broadening of the ^{3}MLCT band in the visible but no lowering of the wavelength of the absorption maximum (see Figure 5a). Partial precipitation was observed for neutral DMPC vesicles. As we suspected that the kinetics of the coordination reaction would be dependent on the concentration of the ligand, we prepared samples B″ (DMPG) and sample E″ (DMPC) by mixing 25 mol % of ligand **4** with the appropriate lipid, preparing the vesicles, and finally (as for B′ and E′) adding 1 mol % of complex $[Ru(terpy)(bpy)(OH_2)]^{2+}$. Upon heating to 70 °C for several hours, DMPC vesicles (sample E″) were not stable and precipitated without appreciable color change. For anionic DMPG vesicles, however, a gradual color change from red to yellow was observed after a few hours. The reaction was followed by UV−vis spectroscopy, which showed that the absorption band at 492 nm gradually disappeared and that a new band appeared around 450 nm, showing the slow formation of a sulfur-bonded ruthenium complex (see Figure 5b). The band at 492 nm did not completely vanish, however, and eight supplementary hours of heating at 70 °C did not improve the situation. Deconvolution of the final spectrum concludes to 63% of sulfur-bound ruthenium complex (see Figure S4 in Supporting Information). We suspect some degradation processes to occur upon heating for a long time (see Discussion). Cryo-TEM pictures were taken from sample B″ after heating (see Figure 6). Unilamellar vesicles and flat discs were still present, which looked similar to the pictures obtained before heating for sample B′ (1 mol % of L). However, some much larger vesicles and flat discs were also observed, with a diameter of up to 500 nm. This is indicative of partial fusion of the lipid bilayers.

Nature of the Flat Discs. The uniform discs observed by cryo-TEM for DMPG vesicles including 1 mol % of complex $[\mathbf{5}]^{2+}$ (sample C) were not present either if the charge of the ruthenium head was removed (sample B or A) or if lipids were used that do not have a net charge (sample D, E or F). In addition, when sample C was irradiated, these structures were conserved, and they were also observed after heating sample B″ at 70 °C, upon

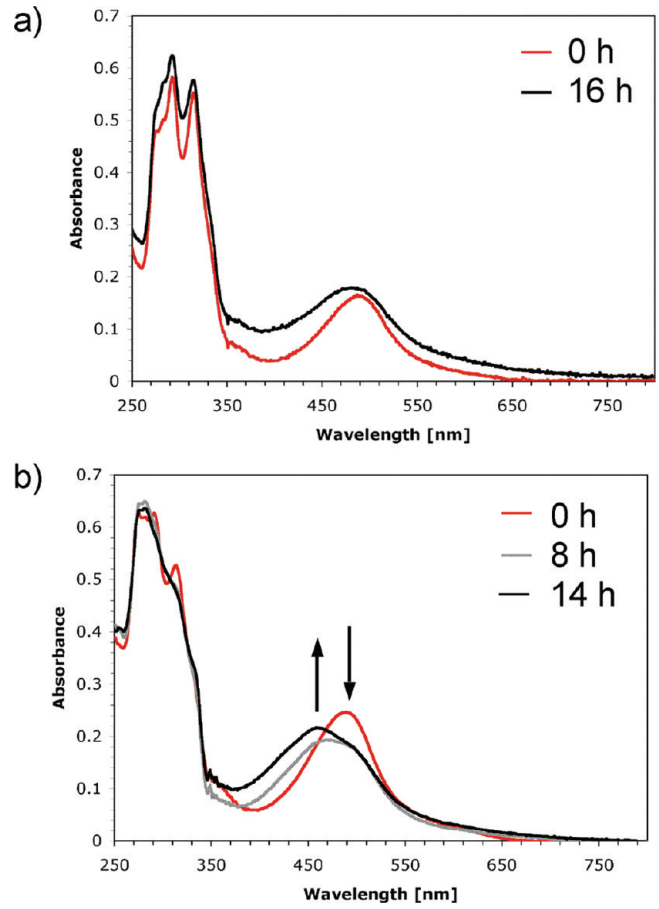

Figure 5. Evolution of the UV−vis spectrum of (a) sample B′ (1 mol % of ligand **4**) after being heated to 80 °C for 16 h and (b) sample B″ (25 mol % of ligand **4**) after being heated to 70 °C for 14 h.

which back binding to the membrane took place. In order to clearly establish the nature of these discs, we tilted the sample holder in the electron microscope. In all cases, the uniform discs and dark lines turn into ovoids, whereas unilamellar vesicles remain spherical (see Figure 7). Reversely, ovoids can be turned into dark lines upon increasing tilt angles (data not shown). Thus, these structures clearly correspond to flat discs that appear differently depending on the observation angle.

Discussion

As recently shown by Hunter et al.,[41] binding and unbinding of transition metal complexes to and from membrane-embedded ligands is an interesting biomimetic approach toward the binding and unbinding of biomolecules at membrane proteins. Usually, metal−steroid conjugates are considered as protein targeting tools because steroids are protein substrates,[42−47] but we are

(41) Dijkstra, H.; Hutchinson, J.; Hunter, C.; Qin, H.; Tomas, S.; Webb, S.; Williams, N. *Chem.—Eur. J.* **2007**, *13*, 7215.
(42) Jackson, A.; Davis, J.; Pither, R.; Rodger, A. *Inorg. Chem.* **2001**, *40*, 3964.
(43) Buil, M. L.; Esteruelas, M. A.; Garces, K.; Onate, E. *Organometallics* **2009**, *28*, 5691.
(44) Jaouen, G.; Vessieres, A.; Butler, I. *Acc. Chem. Res.* **1993**, *26*, 361.
(45) Lo, K. K.-W.; Lee, T. K.-M.; Lau, J. S.-Y.; Poon, W.-L.; Cheng, S.-H. *Inorg. Chem.* **2008**, *47*, 200.
(46) Lo, K. K.-W.; Tsang, K. H.-K.; Sze, K.-S.; Chung, C.-K.; Lee, T. K.-M.; Zhang, K. Y.; Hui, W.-K.; Li, C.-K.; Lau, J. S.-Y.; Ng, D. C.-M.; Zhu, N. *Coord. Chem. Rev.* **2007**, *251*, 2292.
(47) Schobert, R.; Bernhardt, G.; Biersack, B.; Bollwein, S.; Fallahi, M.; Grotemeier, A.; Hammond, G. L. *Chem. Med. Chem.* **2007**, *2*, 333.

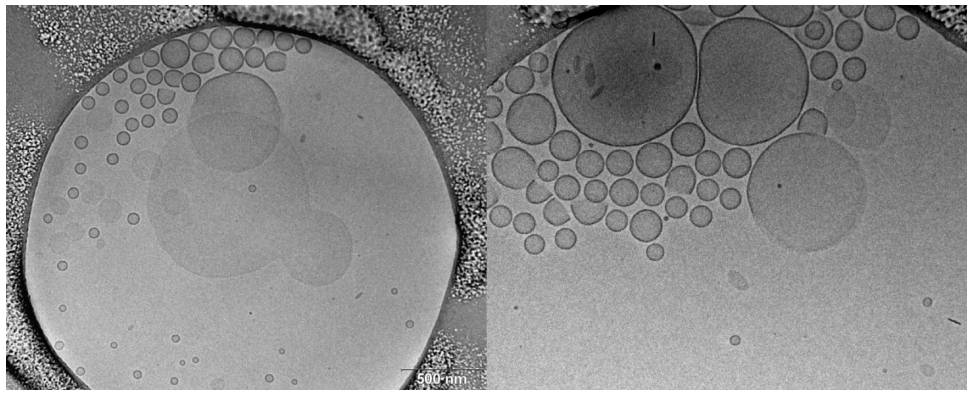

Figure 6. Cryo-TEM pictures of sample B″ after heat treatment at 70 °C for 22 h (B″ = DMPG including 25 mol % of ligand **4**, to which 1 mol % of $[Ru(terpy)(bpy)(OH_2)]^{2+}$ was added).

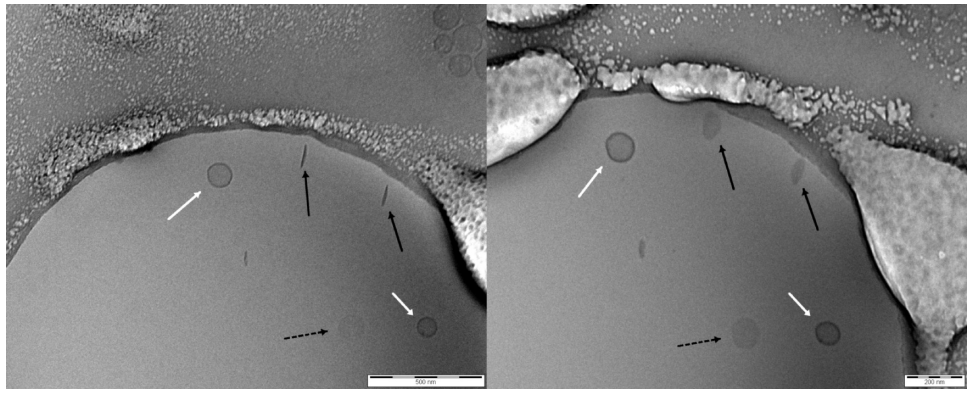

Figure 7. Cryo-TEM pictures of sample C after irradiation at two different tilt angles of the sample holder: $\angle = 0°$ (left) and 30° (right). White arrows, spherical liposomes; black arrows, dark lines (left) turning to ovoids (right) upon tilting; dashed arrows, uniform discs. Similar pictures are observed before irradiation.

using cholesterol derivatives for their ability to insert into biological membranes.[48] By covalently binding a 5α-cholestan-3β-ol fragment to a monodentate thioether ligand and subsequently coordinating **4** to ruthenium, we aimed at decorating unilamellar vesicles with ruthenium polypyridyl complexes. UV−vis spectra of the functionalized DMPG and DMPC vesicles were comparable to the spectrum of $[\mathbf{5}]^{2+}$ in acetone. In addition, the yellow color due to the presence of the sulfur-bonded ruthenium complex significantly diminished upon spinning down the lipid vesicles. Thus, we can conclude that the ruthenium complexes were attached to DMPG and DMPC membrane via (1) direct coordination of the sulfur atom to ruthenium and (2) supramolecular insertion of the cholestanol moiety into the lipid bilayer.

Interestingly, a small (25%) to medium (56%) fraction of S-bound ruthenium complex was also found in the supernatant before irradiation for samples C and F, respectively. As a Rouser assay of the supernatant excludes small unilamellar vesicles that would not be spun down by centrifugation, such minor fraction might be caused by (1) partial hydrolysis of the ester bond in complex $[\mathbf{5}]^{2+}$, which would liberate the partially water-soluble complex $[Ru(terpy)(bpy)(S(Me)CH_2COOH)]^{2+}$, or (2) exchange of the counteranion of complex $[\mathbf{5}]^{2+}$. Indeed, the solubility of complex $[\mathbf{5}]^{2+}$ in water highly depends on its counteranion. During the purification of compound $[\mathbf{5}]^{2+}$ by chromatography, for example, evaporation of acetone from the acetone/water/KNO_3 fractions ($[NO_3]^- \approx 0.032$ M) does not lead to precipitation of the orange complex, unless large amounts of saturated aqueous KPF_6 solution are added. Thus, compound $[\mathbf{5}]^{2+}$ in the nitrate form, i.e., $[\mathbf{5}](NO_3)_2$, is partly soluble in aqueous solution despite its long apolar tail, whereas $[\mathbf{5}](PF_6)_2$ is not. Thus, the lipophilic hexafluorophosphate anions of the complex initially introduced in the vesicle-containing samples might gradually be exchanged by the more hydrophilic hydrogenophosphates or sulfates anions present in the buffer, thus increasing the solubility of complex $[\mathbf{5}]^{2+}$ in aqueous solution, which might explain the amount of complex still present in the supernatant after centrifugation.

The photochemistry of $[Ru(terpy)(N-N)(Y)]^{2+}$, where N−N is a bidentate diimine ligand and Y is a monodentate ligand, has been studied thoroughly in (wet) organic solvents.[17,20,27,32,33,39] However, to our knowledge it is the first time that the selective photosubstitution of Y by an aqua ligand is reported in purely aqueous solution. The presence of clear isosbestic points during irradiation shows that a single photoreaction is taking place. The first-order kinetics also corresponds to previous work, where it was shown that upon ligand photoexpulsion coordination of a solvent molecule is taking place.[18] All the experiments carried out in the present work (UV−vis spectroscopy, TEM, centrifugation) converge to a great similarity between samples C after irradiation and sample B′ on the one hand, and between sample F after irradiation and sample E′ on the other hand (see Table 1). Thus, we conclude that the following reaction is taking place at the membrane:

(48) d'Hardemare, A. D.; Torelli, S.; Serratrice, G.; Pierre, J. L. *Biometals* **2006**, *19*, 349.

$$\{[Ru(terpy)(bpy)(\mathbf{4})^{2+}]\}_{@LUV} \xrightarrow[\substack{pH\ =\ 7.0\\ water,\ r.t..}]{h\nu} [Ru(terpy)(bpy)(OH_2)]^{2+} + \{\mathbf{4}\}_{@LUV}$$

As the cholestanol fragment of **4** is inserted in the membrane, the above reaction should lead to the detachment of the ruthenium complex from the bilayer. As depicted in Figure 8, however, depending on the charge of the lipids, two different situations were found. First, with anionic lipids (DMPG) ultracentrifugation after irradiation leaves a small fraction (∼15%) of the initial absorbance of $[Ru(terpy)(bpy)(OH_2)]^{2+}$ in the supernatant, which accounts for a strong electrostatic interactions between the "free", positively charged ruthenium complex and the negatively charged membrane. On the contrary, with neutral lipids (DMPC) ultracentrifugation after irradiation leaves a large fraction (75−100%) of the initial absorbance of $[Ru(terpy)(bpy)(OH_2)]^{2+}$ in the supernatant, which accounts for a weak interaction between the ruthenium complex and the membrane. As no bias was introduced for incorporation of the complexes in the outer and inner monolayer, one would expect close to 50% of the liberated complexes in the supernatant after centrifugation, if the ruthenium complexes situated inside the vesicles were not able to cross the membrane. Considering the large size of the vesicles, finding significantly more than 50% is an indication that DMPC membranes might be leaky toward $[Ru(terpy)(bpy)(OH_2)]^{2+}$. Two factors might explain such permeability of the membrane toward $[Ru(terpy)(bpy)(OH_2)]^{2+}$. Either the DMPC vesicles have holes because the temperature during ultracentrifugation (25 °C) is close to their phase transition temperature (24 °C), in which case the leakiness is due to the coexistence, at that temperature, of domains that are in the fluid and in the gel phase.[49] Alternatively, $[Ru(terpy)(bpy)(OH_2)]^{2+}$ might be lipophilic enough to cross the membrane by partial solubilitization, which has been recently suggested for related polypyridyl ruthenium(II) complexes.[50,51]

Quantum yield measurements show that photocleavage of the ruthenium complexes from the vesicles is as efficient as comparable homogeneous systems,[17,18] and according to DLS and cryo-TEM analysis it does not change the size or shape of the vesicles themselves. By contrast, thermal coordination of $[Ru(terpy)(bpy)(OH_2)]^{2+}$ to the thioether-decorated vesicles is a slow process, and heating to 70 °C for prolonged times is required to observe partial coordination. DMPC vesicles are not stable under such hard conditions and aggregate into larger particles that ultimately precipitate. For DMPG vesicles repulsive electrostatic interactions between the vesicles prevent precipitation of the vesicles, which allows for the observation of back-coordination by UV−vis spectroscopy. Thus upon heating the following reaction takes place:

$$[Ru(terpy)(bpy)(OH_2)^{2+}] + \{\mathbf{4}\}_{@DMPG} \xrightarrow[pH\ =\ 7.0]{heating} \{Ru(terpy)(bpy)(\mathbf{4})^{2+}\}_{@DMPG}$$

However, cryo-TEM also shows that after heating aggregation of the LUVs have occurred, as much larger vesicles and bicelles are observed. In addition, the remaining shoulder at 492 nm after heating (see Figure 5b) indicates that a minor fraction

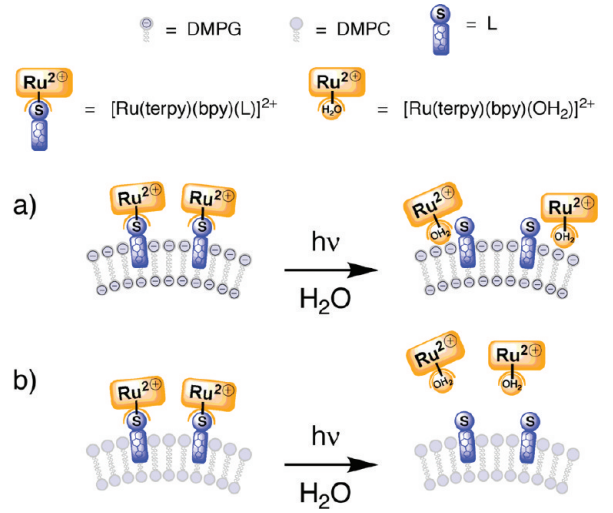

Figure 8. Model for the irradiation of $[\mathbf{5}](PF_6)_2$ at membranes: (a) with anionic DMPG lipids and (b) with neutral DMPC lipids.

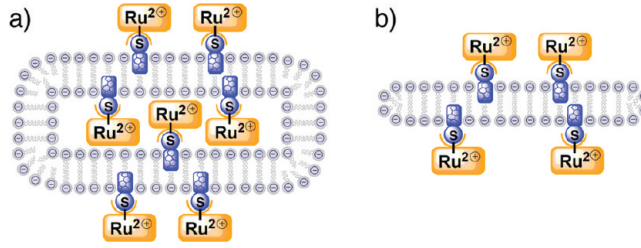

Figure 9. Model for the formation of the "pancakes" observed by cryo-TEM: (a) double bilayers and (b) single bilayers (bicelles).

(≈35%, see deconvolution Figure S4) of ruthenium complexes cannot coordinate to the thioether ligands imbedded in the membrane. The interpretation of this is still unclear; it is not possible to fully exclude degradation processes such as lipid hydrolysis, hydrolysis of the ester linker in ligand **4**, or slow oxidation of the sulfur ligands to sulfoxides or sulfones.

Flat discs made of lipids might either be bilamellar bilayers, i.e., flattened vesicles, or bicelles, i.e., unilamellar lipid discs (see Figure 9). As electrostatic interactions are necessary to observe these discs, we initially considered the first hypothesis, where flattening of the vesicles would be caused by attractive electrostatic interactions between the ruthenium heads situated in the inner monolayer, and the negative lipids facing them at the opposite side of the inner monolayer (Figure 9a). Similar electrostatic interactions are commonly invoked to explain how divalent Ca^{2+} or Mg^{2+} cations stabilize negatively charged lipid bilayers on negatively charged glass or mica surfaces.[52] However, the thickness of the discs was measured under an angle where they appear as black lines. We found only 7 ± 1 nm, which corresponds to single discoidal bilayers, thus bicelles (see Figure 9b). Bicelles were typically described when a combination of very short lipids (typically in C_6) and long lipids (C_{12}−C_{18}) was used, and usually the short lipids concentrate at the rim of the bicelle.[53−55] Our system is deprived of such short lipids, but $[\mathbf{5}]^{2+}$ being composed of a polar head and an apolar

(49) Noordam, P. C.; Killian, A.; Elferink, R. F. M. O.; Degier, J. *Chem. Phys. Lipids* **1982**, *31*, 191.
(50) Schatzschneider, U.; Niesel, J.; Ott, I.; Gust, R.; Alborzinia, H.; Wolfl, S. *Chem. Med. Chem.* **2008**, *3*, 1104.
(51) Zava, O.; Zakeeruddin, S. M.; Danelon, C.; Vogel, H.; Gratzel, M.; Dyson, P. J. *ChemBioChem* **2009**, *10*, 1796.
(52) Richter, R.; Brisson, A. *Biophys. J.* **2005**, *88*, 3422.
(53) Diller, A.; Loudet, C.; Aussenac, F.; Raffard, G.; Fournier, S.; Laguerre, M.; Grelard, A.; Opella, S. J.; Marassi, F. M.; Dufourc, E. J. *Biochimie* **2009**, *91*, 744.
(54) Katsaras, J.; Harroun, T.; Pencer, J.; Nieh, M. *Naturwissenschaften* **2005**, *92*, 355.

cholestanol moiety might behave as a surfactant, which are known to sometimes lead to the formation of bicelles and open vesicles.[56] Very recently, a similar effect has been reported with sulfate-functionalized cholesterols in DMPC/DHPC lipid bilayers.[57]

Conclusion

The present work represents our first attempt of probing the (photo)coordination properties of ruthenium complexes in the biomimetic environment of a lipid bilayer. By synthesizing a cholestanol-thioether hybrid that coordinates to ruthenium via its sulfur atom, we were able to decorate large unilamellar vesicles with ruthenium polypyridyl complexes. When using negatively charged lipids to build up the membrane (DMPG), both electrostatic interactions and insertion of the apolar tail of the ligand into the bilayer seem to play a role in the metal−membrane interaction. After visible light irradiation and cleavage of the Ru−S bond, the free aqua complex $[Ru(terpy)(bpy)(OH_2)]^{2+}$ still interacts with the membrane through electrostatic forces, which allows for back-coordination of the complex to the vesicles, though at high ligand concentrations and elevated temperatures. Increasing the rate of thermal binding to the membrane-embedded ligands is a prerequisite before fast hopping of metal complexes at the surface of a vesicle can be obtained. Ultimately, organization of the ligands at the membrane might allow for light-controlled motion of single molecules at the membrane−water interface.

When neutral lipids were used to build up the membrane (DMPC), insertion of the cholestanol group into the bilayer is the only interaction between the complex and the membrane. After light irradiation and cleavage of the Ru−S bond, the photoproduct $[Ru(terpy)(bpy)(OH_2)]^{2+}$ diffuses away in solution, which might allow for delivering a potentially biologically active compound. In parallel to phototherapy[58] and photodynamic therapy,[59−61] light activation[62−64] and light-triggered delivery[65−67] of metal drugs represent fast-developing research fields. Our system combines a photocleavable metal complex and lipid bilayers as biocompatible carriers.[68−72] It represents thus a potentially new alternative to introduce drugs in the body, where the drug is attached to the membrane itself by a photocleavable coordination bond, instead of being encapsulated into it.[73,74]

Acknowledgment. The Dutch Organization for Scientific Research (NWO-CW/Vernieuwingsimpuls) is kindly acknowledged for a Veni grant to S.B.

Supporting Information Available: Evolution of the absorbance of vesicle solutions during quantum yield measurement, actinometry data, and deconvolution of the spectrum after heating (shown in Figure 5b). This material is available free of charge via the Internet at http://pubs.acs.org.

JA105025M

(55) Prosser, R. S.; Evanics, F.; Kitevski, J. L.; Al-Abdul-Wahid, M. S. *Biochemistry* **2006**, *45*, 8453.
(56) Visscher, I.; Stuart, M.; Engberts, J. *Org. Biomol. Chem.* **2006**, *4*, 707.
(57) Shapiro, R. A.; Brindley, A. J.; Martin, R. W. *J. Am. Chem. Soc.* **2010**, *132*, 11406.
(58) Schneider, L. A.; Hinrichs, R.; Scharffetter-Kochanek, K. *Clin. Dermatol.* **2008**, *26*, 464.
(59) O'Connor, A. E.; Gallagher, W. M.; Byrne, A. T. *Photochem. Photobiol.* **2009**, *85*, 1053.
(60) Ogura, S.-i.; Tabata, K.; Fukushima, K.; Kamachi, T.; Okura, I. *J. Porphyrins Phthalocyanines* **2006**, *10*, 1116.
(61) Ortel, B.; Shea, C. R.; Calzavara-Pinton, P. *Front. Biosci.* **2009**, *14*, 4157.
(62) Bednarski, P.; Grunert, R.; Zielzki, M.; Wellner, A.; Mackay, F.; Sadler, P. *Chem. Biol.* **2006**, *13*, 61.
(63) Heringova, P.; Woods, J.; Mackay, F. S.; Kasparkova, J.; Sadler, P. J.; Brabec, V. *J. Med. Chem.* **2006**, *49*, 7792.
(64) Mackay, F.; Woods, J.; Moseley, H.; Ferguson, J.; Dawson, A.; Parsons, S.; Sadler, P. *Chem.—Eur. J.* **2006**, *12*, 3155.
(65) Alvarez-Lorenzo, C.; Bromberg, L.; Concheiro, A. *Photochem. Photobiol.* **2009**, *85*, 848.
(66) Gerasimov, O. V.; Boomer, J. A.; Qualls, M. M.; Thompson, D. H. *Adv. Drug Delivery Rev.* **1999**, *38*, 317.
(67) Zeimer, R.; Goldberg, M. F. *Adv. Drug Delivery Rev.* **2001**, *52*, 49.
(68) Abraham, S.; Edwards, K.; Karlsson, G.; MacIntosh, S.; Mayer, L.; McKenzie, C.; Bally, M. *Biochim. Biophys. Acta, Biomembr.* **2002**, *1565*, 41.
(69) Cui, J.; Li, C.; Wang, L.; Wang, C.; Yang, H.; Li, Y.; Zhang, L.; Zhang, L.; Guo, W.; Liang, M. *Int. J. Pharm.* **2009**, *368*, 24.
(70) Storrs, R. W.; Tropper, F. D.; Li, H. Y.; Song, C. K.; Kuniyoshi, J. K.; Sipkins, D. A.; Li, K. C. P.; Bednarski, M. D. *J. Am. Chem. Soc.* **1995**, *117*, 7301.
(71) Taggar, A. S.; Alnajim, J.; Anantha, M.; Thomas, A.; Webb, M.; Ramsay, E.; Bally, M. B. *J. Controlled Release* **2006**, *114*, 78.
(72) Torchilin, V. *Adv. Drug Delivery Rev.* **1997**, *24*, 301.
(73) Chupin, V.; de Kroon, A.; de Kruijff, B. *J. Am. Chem. Soc.* **2004**, *126*, 13816.
(74) Hamelers, I. H. L.; De Kroon, A. I. P. M. *J. Liposome Res.* **2007**, *17*, 183.